An Embedded Atom Method for Alloy Nanoparticles

Bin Shan, Jangsuk Hyun, Ligen Wang, Sang Yang, Neeti Kapur, and John B Nicholas
Nanostellar Inc
3696 Haven Ave, Redwood City, CA, USA, jnicholas@nanostellar.com

ABSTRACT

One of the key problems in studying nanoparticles is the characterization of their segregation behavior. We present here the development and application of a high-accuracy embedded atom method (EAM) potential for the simulation of metal alloy nanoparticles. The potential was parameterized by a large set of density functional theory (DFT) calculations of metal nanoparticles in addition to bulk properties. The EAM potential accurately reproduces heats of formation, bulk moduli, chemical potentials and geometries. We used this EAM potential in Monte Carlo simulations of PdAu nanoparticles ranging from 55-atoms ($\sim$ 1nm) to 5083-atom particles ($\sim$ 5nm). The potential can be utilized for computational screening of different binary and ternary alloy particles for catalysis.

Keywords: embedded atom method, PdAu, alloy, segregation, catalyst

1 Introduction

Metal alloy nanoparticles have been widely used in many industries, including electronics and catalysis. Their large surface to bulk ratio, as well as their quantum confinement effects, make nanoparticles attractive for many potential applications [1]. Despite their appealing properties, the average number of atoms in a particle usually goes well beyond a thousand, making direct first-principles density functional theory (DFT) calculations prohibitively expensive [2].

Over the years, many empirical potentials and force fields have emerged for modeling large numbers of atoms and molecules [3]–[6]. The empirical methods ignore the fast movement of the electrons and only deal with the slower movement of atom and ions, thus providing a highly effective means of predicting the energetic and structural properties of nanoparticles. The Embedded Atom Method (EAM) is one of the most successful in describing metallic systems [3]. However, most previous work has focused on the study of bulk behavior and the parameterized EAM potentials generally do not faithfully reproduce nanocluster behavior. Recently, some efforts has been made toward this direction by including additional parameters that reflect the local asymmetric charge distribution [7].

In this paper, we report the development, parameterization, and application of an EAM potential that is benchmarked to state-of-the-art DFT calculations. To parameterize potentials that are accurate for nanoparticles, we calculated standard bulk properties, such as rose curves, sheer distortions, and surface energies, as well as the energies of 3 to 147-atom clusters, all within DFT framework at the Perdew-Burke-Erzernhof functional (PBE) level [11]. The parameterized EAM potentials of the pure metals reproduce faithfully both bulk properties and cluster geometries and energies. The parameterized cross-pair potentials for alloys agree well with heats of formation, and maintain the correct energy ordering of the alloy nanoparticles under different segregation configurations. As an example of the utilization of our EAM potential, we carried out Monte-Carlo (MC) simulations of PdAu alloy nanoparticles ranging from 55 to 5083 atoms. We demonstrate how different factors like temperature, particle size, and the alloy composition ratio influence the surface morphology of the nanoparticle. Our computational study provides a comprehensive dataset of alloy nanoparticle segregation behavior that gives insight into catalyst characterization and identification.

2 Computational Methods

We briefly describe in the following sections the procedures we used in the DFT calculations, the EAM parameterization for pure elements, the cross-pair potential fitting, and the MC simulations of PdAu nanoparticles.

2.1 EAM for Pure Elements

Conceptually, the total energy of a given system within the EAM framework can be expressed as

$$E_{tot}(\rho) = F(\rho) + \sum_{i<j} \phi(r_i, r_j) \qquad (1)$$

where the first term is the embedding function representing the energy of embedding an atom in a free electron sea of density ρ, while the second term is a correction term in the form of pair-wise interactions between

NSTI-Nanotech 2008, www.nsti.org, ISBN 978-1-4200-8503-7 Vol. 1

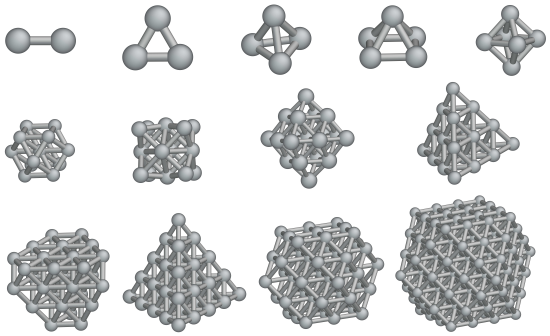

Figure 1: Clusters that are included in the parameterization of EAM. They are Pd_2, Pd_3, Pd_4, Pd_5, Pd_6, Pd_{13}, Pd_{14}, Pd_{19}, Pd_{20}, Pd_{31}, Pd_{35}, Pd_{55}, Pd_{147}, respectively

neighboring atoms located at r_i and r_j. Such empirical potentials avoid solving the electronic wavefunction and are capable of handling much larger systems than quantum mechanical calculations. Many different types of embedding functionals and pair-wise interactions have been proposed to give an accurate estimate of the total energy of the system [5], [8]–[10]. We have based our work on Zhou's scheme where spline functions were used to interpolate the embedding functions at different charge density regions [9], [12]. To add additional flexibility to the EAM potential, especially the low electron density range, which usually occurs in coordinately unsaturated atoms, we added additional splines.

In addition to the bulk properties that EAM potentials are commonly parameterized against, such as cohesive energies, rose curves, sheer distortions and surface energies, we have included in our fit a series of nanoparticles to improve the quality of our EAM potential. Figure 1 shows an example of 13 Pd cluster geometries that was included in the parameterization of Pd potential. All geometries of the clusters were optimized by DFT and their binding energies were obtained. Both the relaxed and un-relaxed geometries were used in the parameterization. The relaxation and total energy calculations were done using the Vienna ab initio simulation package [13] with the PBE exchange-correlation functional [11].

Figure 2 shows the comparison between DFT data and EAM results for Pd bulk properties and nanoparticle binding energies. The parameterized potential not only reproduces all the bulk properties, but also accurately maps the binding energies of different-sized clusters. We followed the same protocol in fitting the EAM potential for Au. In both cases, the correlation coefficient (R^2) between DFT data and EAM prediction is larger than 0.98, indicating excellent correlation.

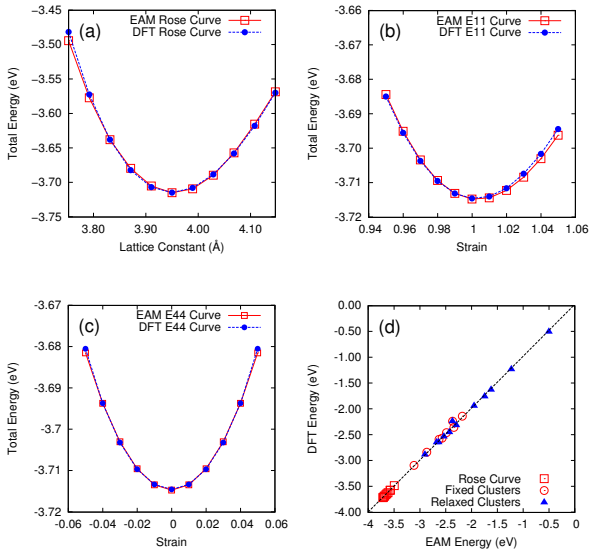

Figure 2: A comparison between DFT and EAM predictions. a) Rose Curve. b) Elastic constant E_{11}. c) Elastic constant E_{44}. d) Binding Energies for clusters.

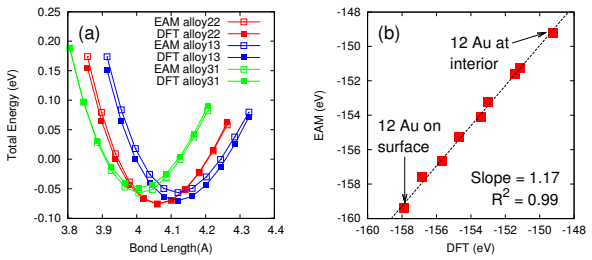

Figure 3: a) The alloy heat of formation for PdAu alloy in 1:3, 2:2, and 3:1 ratio. b) Correlation between DFT and EAM for $Pd_{43}Au_{12}$ nanoparticles with different segregation profiles.

2.2 Cross Pair for Alloys

We used the same functional form as Zhou's pairwise potential for the cross pair potential [9], [12], but have re-parameterized the pair potential to the DFT heat of formation for PdAu alloys with 3:1, 2:2, and 1:3 composition ratios. Figure 3 demonstrates the excellent correlation between the DFT heat of formation curve as a function of lattice constant.

We have also validated the accuracy of the cross pair by comparing the energies of a 55-atom $Pd_{43}Au_{12}$ nanoparticles with different segregation profiles. The top right point on figure 3b corresponds to the $Pd_{43}Au_{12}$ particle where 12 Au atoms are all segregated to the surface, while the left bottom point represents the case where 12 Au atoms are in the interior of the nanoparticle. The points in between represents intermediate states where some Au has segregated to the surface. The

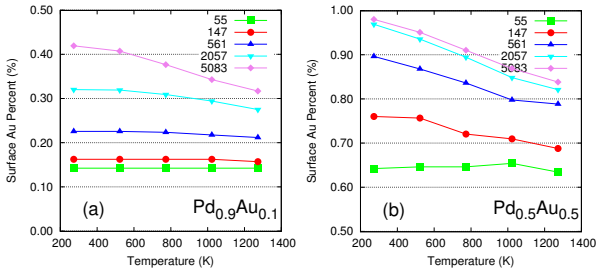

Figure 4: Segregation behavior as a function of temperature for different sized PdAu nanoparticles a) Pd rich nanoparticle. b) 1:1 ratio PdAu nanoparticle.

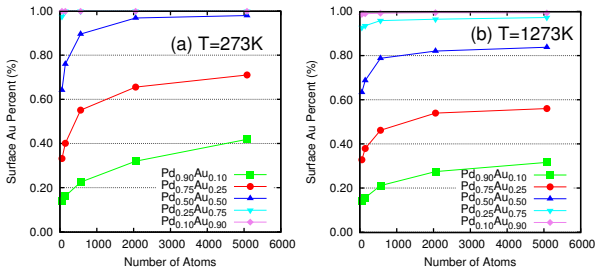

Figure 5: Segregation behavior as a function of particle size (a) at T=273K (b) at T=1273K

energy ordering between particles with different segregation profiles is in exact agreement with DFT result.

2.3 Monte-Carlo Simulations

In order to probe the equilibrium properties of PdAu nanoparticles, we used MC simulations with the Metropolis algorithm [14]. The simulations were run for PdAu nanoparticles with different composition ratios ($Pd_{0.9}Au_{0.1}$, $Pd_{0.75}Au_{0.25}$, $Pd_{0.5}Au_{0.5}$, $Pd_{0.25}Au_{0.75}$, $Pd_{0.1}Au_{0.9}$), different particle sizes (55, 147, 561, 2057, 5083 atoms) and at different temperatures (273K, 523K, 773K, 1023K, 1273K). A random swap of two atoms fixed on the lattice is attempted and is either accepted or rejected according the the Metropolis rule [14]. This procedure is repeated for over one million steps for each of the cases we studied. The final morphology of the particle is obtained by taking a statistical average of the last 10000 steps, after the particle has reached equilibrium.

3 Results and Discussions

Since the surface energy of Au is smaller than that of Pd, we expect that Au atoms will segregate to the particle surface to minimize the total energy of the system. A compensating effect is the negative heat of formation of the PdAu alloy, which tends to promote PdAu mixing rather than keeping the elements totally separated. These two competing mechanisms determine the final morphology of the nanoparticle. In the following sections, we discuss how different factors, including temperature, particle size and composition ratios, would change the surface concentration of Au in a PdAu alloy.

3.1 Segregation vs Temperature

Figure 4 shows the effect of temperature on the surface morphologies of PdAu nanoparticles. Figure 4a is for a Pd rich alloy ($Pd_{0.9}Au_{0.1}$), and Figure 4b is for PdAu with 1:1 composition ratio. Layer by layer osillation in concentration is generally observed, where the outmost layer is Au rich while the sub-layer is Pd rich. For the current study, we focus on the surface layer only and analyze how the Au concentration changes with different factors. It can be seen that the the surface concentration of Au is significantly enriched as compared to its bulk composition ratio, and the surface composition of small particles is very resistant to temperature change. This effect is primarily due to the fact that small nanoparticles are dominated by vertex and edge sites, where Au and Pd atoms have significant energy differences. Even the highest temperature we studied (1273K) is unable to invert the surface Au concentration. For larger nanoparticles however, we do see a significant decrease in surface Au concentration with higher temperature. The surface Au concentration change with respect to temperature is most significant for PdAu alloys with Au concentration in the 25% to 50% range. Larger Au concentrations lead to an Au-dominated surface irrespective of temperature, while for smaller Au concentrations, the change is limited by the amount of Au available.

3.2 Segregation vs Particle Size

Figure 5 shows the surface segregation versus particle size at T=273K and T=1273K, respectively. For Au rich nanoparticles, the surface forms a monolayer of Au. In the Pd rich particles, we see an initial sharp increase in the Au concentration followed by an asymptotic plateau. For each series of curves with same color, the PdAu composition ratio is kept fixed. Thus, smaller nanoparticles having larger surface-to-volume ratios develop a smaller Au surface concentration. This is the main reason for the slope change in Au concentration versus particle size. If we make the assumption that the maximum number of surface Au atoms is limited by the number of Au atoms in the alloy, which is true for Pd rich alloys under lower temperature, we expect the surface Au concentration will follow a $N^{1/3}$ curve with respect to the total number of atoms. This qualitatively agrees with what we see in the lower portion of Figure 5.

3.3 Segregation vs Particle Composition

We finally discuss the segregation behavior with respect to the Pd:Au composition ratio (Figure 6). The

NSTI-Nanotech 2008, www.nsti.org, ISBN 978-1-4200-8503-7 Vol. 1

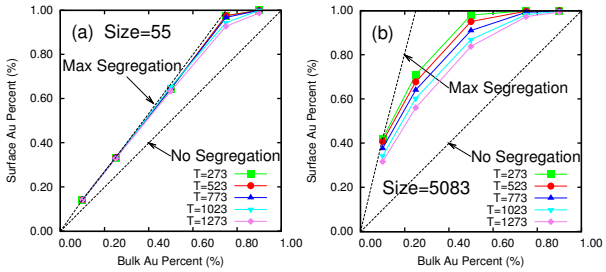

Figure 6: Segregation behavior as a function of Au composition for a) 55-atom particle. b) 5083-atom particle.

diagonal line across the graph indicates the case of no segregation while the other dotted line shows the maximum possible degree of segregation as permitted by the number of available Au atoms in the particle. It is clear from the graph that for small size nanoparticles, the Au atoms segregate under all temperatures. Au continues segregating to the surface until it reaches a full monolayer. The degree of segregation is less pronounced in larger nanoparticles, where the negative heat of formation of PdAu keeps a fraction of Au inside the nanoparticle to maintain the energetically favorable equilibrium structure. It can also be seen that the segregation of Au is less pronounced at higher temperatures.

4 Conclusions

We have developed and parameterized a set of EAM potentials for the modeling of alloy nanoparticles. These potentials yield accurate results for both bulk properties and nanoparticle geometries and energies. We used the EAM potential to study the segregation behavior of PdAu nanoparticles with different sizes, composition ratios, and at different temperatures. Our MC simulation indicates an almost full segregation of Au to the surface in small nanoparticles. In large nanoparticles, especially for lower Au concentrations, a temperature dependent Au surface segregation is observed. The influence of different factors on segregation that has been presented here gives insight into PdAu nanoparticle morphology.

REFERENCES

[1] C. Burda, X. Chen, R. Narayanan, and M.A. El-Sayed, Chem. Rev. 105, 1025 (2005).
[2] W. Kohn, Rev. Mod. Phys. 71, 1253 (1999).
[3] M.S. Daw and M. I. Baskes, Phys. Rev. B 29, 6443 (1984).
[4] A.P. Sutton and J. Chen, Phil. Mag. Lett. 61, 139 (1990).
[5] R.A. Johnson, Phys. Rev. B 39, 12554 (1989).
[6] D.W. Brenner, Phys. Rev. B 42, 9458 (1990).
[7] B. Lee and K. Cho, Surf. Sci 15, 1982 (2006).
[8] J. Cai and Y.Y. Ye, Phys. Rev. B 54, 8398 (1996).
[9] X.W. Zhou, R. A. Johnson, and H.N.G. Wadley, Phys. Rev. B 69, 144113 (2004).
[10] H.R. Gong, L.T. Kong, W.S. Lai, and B.X. Liu, Phys. Rev. B 66, 104204 (2002).
[11] J.P. Perdew, K. Burke, and M. Ernzerhof, Phys. Rev. Lett. 77, 3865 (1996).
[12] H.N.G Wadley, X. Zhou, R.A. Johnson, and M. Neurock, Prog. Mat. Sci. 46, 329 (2001).
[13] G. Kresse, J. Furthemuller, Comp. Mat. Sci. 6, 15 (1996).
[14] N. Metropolis, A.W. Rosenbluth, M.N. Rosenbluth, A.H. Teller, and E. Teller, J. Chem. Phys. 21, 1087 (1953).